environments

Article

NOx and CO Fluctuations in a Busy Street Canyon

Peter Brimblecombe [1,*], Meng-Yuan Chu [2], Chun-Ho Liu [3] and Zhi Ning [2]

[1] Department of Marine Environment and Engineering, National Sun Yat-Sen University, Kaohsiung 80424, Taiwan
[2] Division of Environment and Sustainability, The Hong Kong University of Science and Technology, Hong Kong, China; mchuaf@connect.ust.hk (M.-Y.C.); ning.hkust@gmail.com (Z.N.)
[3] Department of Mechanical Engineering, The University of Hong Kong, Hong Kong, China; chliu@hku.hk
* Correspondence: p.brimblecombe@uea.ac.uk

Abstract: Busy street canyons can have a large flow of vehicles and reduced air exchange and wind speeds at street level, exposing pedestrians to high pollutant concentrations. The airflow tended to move with vehicles along the canyon and the 1-s concentrations of NO, NO_2 and CO were highly skewed close to the road and more normally distributed at sensors some metres above the road. The pollutants were more autocorrelated at these elevated sensors, suggesting a less variable concentration away from traffic in the areas of low turbulence. The kerbside concentrations also showed cyclic changes approximating nearby traffic signal timing. The cross-correlation between the concentration measurements suggested that the variation moved at vehicle speed along the canyon, but slower vertically. The concentrations of NOx and CO were slightly higher at wind speeds of under a metre per second. The local ozone concentrations had little effect on the proportion of NOx present as NO_2. Pedestrians on the roadside would be unlikely to exceed the USEPA hourly guideline value for NO_2 of 100 ppb. Across the campaign period, 100 individual minutes exceeded the guidelines, though the effect of short-term, high-concentration exposures is not well understood. Tram stops at the carriageway divider are places where longer exposures to higher levels of traffic-associated pollutants are possible.

Keywords: NO_2; traffic emissions; traffic lights; kerbside environment; roadside exposure; Hong Kong

Citation: Brimblecombe, P.; Chu, M.-Y.; Liu, C.-H.; Ning, Z. NOx and CO Fluctuations in a Busy Street Canyon. *Environments* **2021**, *8*, 137. https://doi.org/10.3390/environments8120137

Academic Editor: Yu-Pin Lin

Received: 4 December 2021
Accepted: 13 December 2021
Published: 15 December 2021

1. Introduction

Deep urban canyons are commonly found in major cities. These are places where limited air exchange leads to poor air quality [1], regardless of the wide range of turbulence-induced fluctuating concentrations [2]. At the base of the canyon, the wind speeds can be low, even if the traffic-generated turbulence is strong. Architectural features, such as advertising signage, overhead walkways [3] and a range of street features [4] such as bus shelters [5] and roadside vegetation [6–8], inhibit the airflows. The ventilation within the canyon may be suppressed [9], and vortices can leave dead zones with stagnant air [2]. Sometimes, slow-moving, heavy traffic along the roads at the canyon bottom exhausts large amounts of primary pollutants and generates turbulence [10]. Typically, ozone (O_3) is a limiting factor for the oxidation of nitric oxide (NO) to nitrogen dioxide (NO_2) [11], making the contribution of primary NO_2 important.

The traffic at the canyon bottom can be dense and persistent, so pedestrians are exposed to elevated pollutant levels even though the dwell time of individuals is often short. Roadside exposure is a concern because people may need to wait to catch buses, taxis or trams, and for others it is a place of work. Roadside air quality is further complicated by diversified transport processes including pulses of pollutant exhaust from passing vehicles, rapid ozone titration or particle formation, resulting in the high variability of field measurement data.

In Hong Kong (HK), 16% of NOx and 50% of CO arise from the road transport sector [12,13]. Quantifying the emissions is therefore crucial to policy formulation for air

quality and public health. It is especially important in urban canyons [14] due to frequent large diesel buses in the city centre [12]. The city has busy, dense, congested road and street canyons with crowded roadside pavements. A large percentage of the population live, work and commute in places strongly affected by traffic-derived air pollutants. These sources are dominated by buses and goods vehicles [15], as private vehicle ownership is comparatively low. In 2019, there were around 76.3 private cars per 1000 people. Hence, the focus is on reducing emissions from high-emitting vehicles with the creation of Franchised Bus Low Emission Zones, where the Euro V standard applies [16]. Central Hong Kong has tall buildings that trap pollutants within street canyons, leading to elevated pollutant concentrations and potentially high exposures [9,17].

Most studies model the full depth of circulation within the urban canyon. Here, we are interested in measurements close to the canyon bottom (i.e., <5 m above ground level). This study deployed multiple high-time-resolution sensors, at 1-s resolution, near congested lanes of traffic in a street canyon in Causeway Bay, HK. These roadside measurements were helpful in determining the nature of short-term variations in the concentration of NO, NO_2 and CO that depict the spatiotemporal variability of the roadside pollutants. This study contributes to the assessment of pedestrian exposure in this heterogeneous environment.

2. Materials and Methods

2.1. Site

The roadside measurements were conducted in Hennessy Road, Causeway Bay (Figure 1a), over the period 09:00–21:00 on four working days, 21 December 2020, 22 December 2020, 28 December 2020 and 29 December 2020 (dates, times and durations in this paper follow ISO 8601). Figure 1b shows the location of the sensor nodes. Figure 1c is a schematic of the roadside deployment. The campaign took place during the COVID-19 pandemic. Although Hong Kong was not under a tight lockdown, restrictions were in place (e.g., restaurants were required to close at 18:00). Under these circumstances, traffic flows may have been slightly reduced during the sampling periods. The sample site was located in a deep canyon (Figure 1d) where buildings on either side of the dual-lane carriageway ranged between 20 and 40 stories (~120–220 m). The sensors were installed along the lanes of the carriageway (eastbound). Along the left of the site were tall buildings, while the other boundary was flanked by a tramway station and footbridge stairs. An overhead walkway runs across the carriageway just before the site. The northern side of Hennessy Road was thus relatively confined at this point, and the electric tramway limited effects from the counter-flowing traffic. The site was about 200 m west of the Causeway Bay Air Quality Station maintained by the Hong Kong Environmental Protection Department (HKEPD). The station has a sample inlet ~3 m above the ground and is ~6 m from the nearest traffic lane.

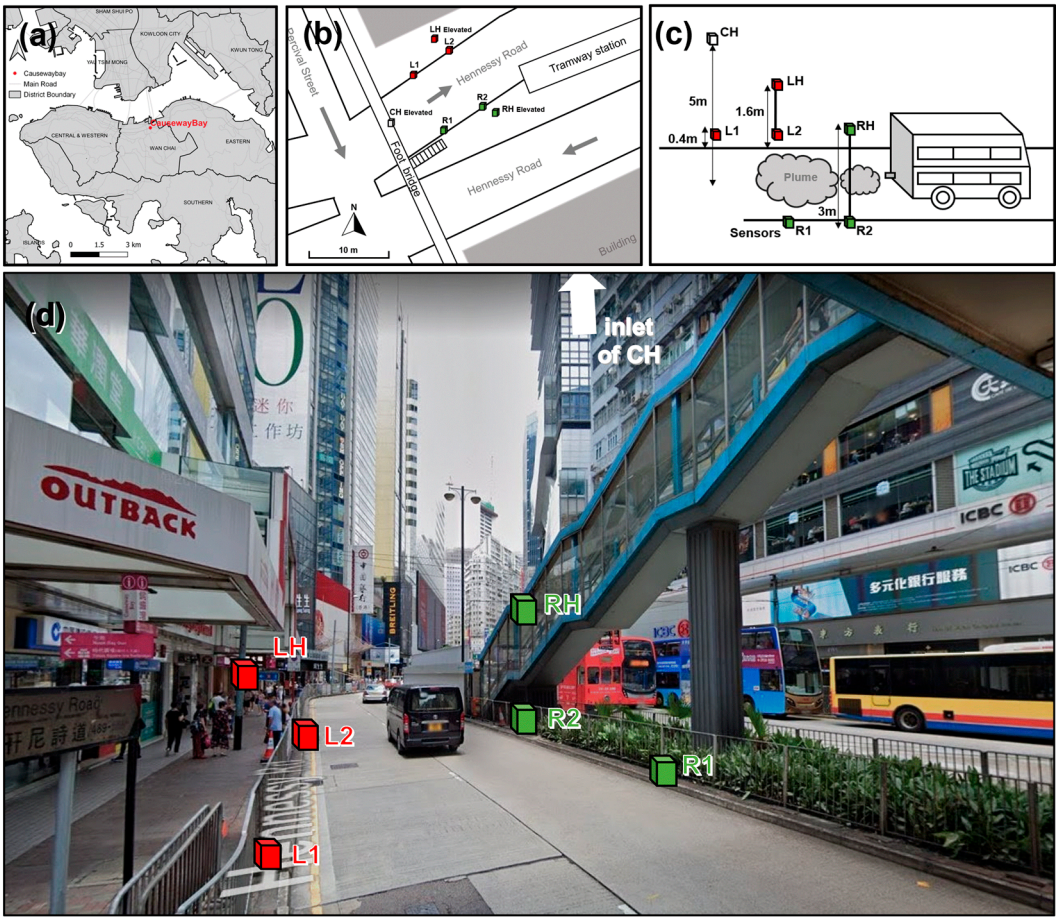

Figure 1. (**a**) Location map showing Causeway Bay on the northern part of Hong Kong Island. (**b**) Layout of the site at Causeway Bay. (**c**) Positions of the sensor nodes. (**d**) Photograph illustrating the site on Hennessy Road, looking east (© Google, June 2019). Tall buildings create an urban canyon and a canopy (OUTBACK) over L1, which shelters pedestrians on the pavement. A tram track (a red tram is partially obscured by the lower end of the staircase) separates the counter-flowing traffic (here seen as buses). At the top right, a portion of the overhead walkway is apparent, where node RH was installed.

Seven High Speed Sensors (HSS-100, Sapiens) were positioned on both sides of the carriageway to capture as much of the exhaust plume as possible and at slightly elevated locations to be more representative of air quality at the canyon bottom (Figure 1c). The measurements were made at the kerb on the left (L1 under a low-rise canopy near the crossroad with Percival Street and further east, L2), and at the kerb of the right lane of the carriageway (R1 and R2). The sensors at the kerb were ~40 cm above the ground, which was close to tailpipe height. The left lane was blocked during the campaign, so all the traffic travelled along the right lane only. The elevated sensor nodes (denoted H for high) were: (i) on the lamp post LH on the left, close to Exit B of the Causeway Bay Mass Transit Railway (MTR) Station, (ii) on the exterior of the overhead pedestrian walkway over the centre of the carriageway CH and (iii) on the right, outside the stairway that provides access to the tram stop RH (Figure 1d). These nodes were all away from the vehicular pollutant sources and elevated above the kerb. Figures 2–6 in this paper adopt the nautical tradition, with the colour red assigned to nodes on the left and green to those on the right.

2.2. Instrumentation

The high-speed sensors have been used in a number of studies at this site [15] and allow continuous measurements of NO, NO_2 and CO at 1-s resolution. They consist of A-Type 4-electrode sensors, which record the raw signal along with corresponding

proprietary baseline sensors to establish the baseline signal (Table 1), using a paired differential filter technology (PDF; patent pending), which reduces sensitivity to humidity and temperature [18]. The kit is small (205 mm × 160 mm × 90 mm), lightweight (<1150 g) and includes a pump for active sampling. An on-board microprocessor captured the rapidly changing pollutant concentrations at the kerb, which were transmitted to a local server by a Wi-Fi module. The internal clocks at each sampling node were synchronised before the deployment. Pollutant concentrations were beyond those normally encountered in urban areas (i.e., NOx > 1000 ppb and CO > 10,000 ppb), as the sensors were deployed right at the kerb. Ultrasonic wind sensors were associated with the monitoring nodes at three locations: near the crossroad (L1), the left side (L2) and the right side (L2). Wind speed and direction were recorded at 1-s resolution (specifications listed in Table 1).

Table 1. Technical details for the monitoring equipment.

	NO	**NO_2**	**CO**	**Wind Sensor**
Sensor	Alphasense NO-A4	Alphasense NO2-A43F	Alphasense CO-A4	Hongyue HY-WDC5
Measurement range	0~20,000 ppb	0~8000 ppb	0~20 ppm	0–40 $m \cdot s^{-1}$ (0–359°)
Resolution	≤1 ppb	≤1 ppb	≤0.01 ppm	0.1 $m \cdot s^{-1}$ (1°)
Noise	<20 ppb	<10 ppb	<20 ppb	3% (3°)
Zero drift in laboratory air	0~50 $ppb \cdot a^{-1}$	0~20 $ppb \cdot a^{-1}$	<±100 $ppb \cdot a^{-1}$	/
Lower detection limit	5 ppb	5 ppb	5 ppb	0.1 $m \cdot s^{-1}$
Response time, T_{50}	≤10 s	≤10 s	≤15 s	/

2.3. Sensor Calibration and QA/QC

Laboratory calibration of the pollutant sensors took place before and after the measurements. Standard CO (100 ppm CO and 10% CO_2/N_2, Linde HKO Ltd., Hong Kong, China) concentrations came from a dynamic calibrator (T700U, Teledyne, Sauzend Oaks, CA, USA) combined with a zero-gas generator (701, Teledyne, Sauzend Oaks, CA, USA). The NO_2 and NO were generated with a $NO_2/NO/O_3$ calibration source (714, 2B Technology, Boulder, CO, USA). During calibration and linearity checks, the gas flow rate was constant at 1 L min^{-1}, which was validated by a flow meter (Defender 520, Mesa Labs, Lakewood, CO, USA). Prior to the calibrations, both the T700U and 2B 714 instruments were warmed up for 30 min, while the pollutant sensors were warmed up for 12 h to ensure a steady state. In addition to local storage (backup), real-time, direct output of pollutant concentrations and system status data were transmitted to a cloud server for online data processing.

2.4. Data Analysis

The data of pollutant concentrations and wind speed were often highly skewed, so the Weibull distribution with the probability density function (f),

$$f = (k/\lambda)(x/\lambda)^{(k-1)} \exp\{-(x/\lambda)^k\}$$

was adopted, where k is the shape parameter, λ the scale parameter and x the variable. Maximum-likelihood fitting to the Weibull distribution was performed by the scipy library of Python. Despite the skewed data, parametric statistical tests were used in this study because the number of observations was large (~150,000 data points from each node), such that the central limit should make parametric methods, such as ANOVA, valid. In cases where the sample size was small (e.g., estimates of lags between sensors), medians and lower (Q_1) and upper quartiles (Q_3) were used to describe the central tendency and dispersion. Autocorrelation and cross-correlation used the online calculator Wessa [19] to explore the time series. Fourier analysis required continuous data and the *SCILAB* Fast Fourier Transform (FFT) was used. Gaps and missing data were often just seconds long, and so were filled via linear interpolation, although the Lomb–Scargle algorithm would be more robust.

3. Results and Discussion

3.1. Wind

As the aspect ratio (building height/street width) increases to ~2.0, a pair of weak counter-rotating secondary vortices are observed at street level [2]. Deep canyons have two or even three weak vortices at the bottom [20]. If the vortices are weak at the canyon bottom, the airflow can be dominated by other processes, such as vehicles or the prevailing wind along the street axis [21]. The wind speeds measured at the site were low. In particular, more than a third of the cases at nodes R2 and L2 were calm wind (after eliminating the missing data). The median and Q_3 were 0.6 and 1.2 m·s^{-1} at node R2 and 0.5 and 1.15 m·s^{-1} at node L2; there was little hint of any notable difference, despite the proximity of the sensor at node R2 to the vehicle wakes. At the site, the most frequent wind direction was along-canyon-axis at node L2 (Figure 2a), which showed the overall wind run at 1-degree intervals over the four days of the campaign. An along-canyon flow was also observed at node R2 (Figure 2b), which could have been caused by the southwest-travelling traffic nearby. The wind pattern at node L1 was similar, but the data are not presented here, because of the potential interference from the nearby crossroad and the shallow canopy.

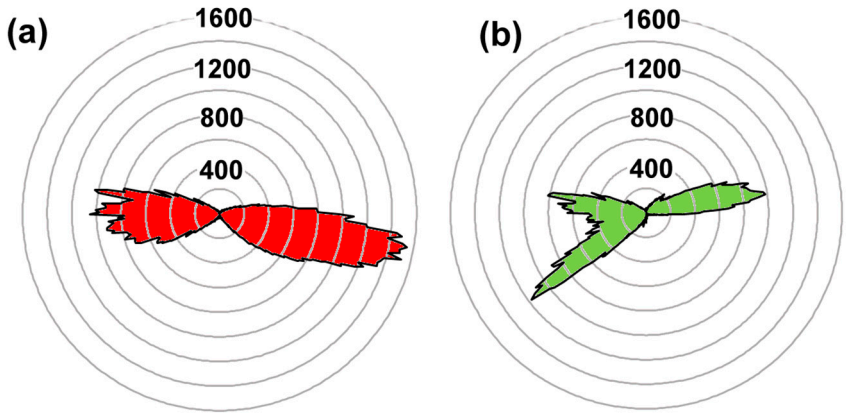

Figure 2. (**a**) Wind vector or metres of wind run over the 4-day campaign at node L2 and (**b**) node R2. Note: the scale is in metres.

3.2. Pollutant Concentrations

The typical measurements of NOx concentrations are shown in Figure 3a, from both the kerbside sensor at the node on the right (R2) and that on the streetside lamp post (LH). The data were filtered with a 15-min moving average and are plotted at 1-min intervals, along with the standard deviation smoothed across the same period. Even with the smoothing, the time traces of the concentrations showed a high level of variability. At the roadside node R2, the variability was driven not only by turbulence but also by the pulses of pollutants from individual vehicles or through longer periods of traffic congestion. The data at 1-s resolution reveal distinct plume segments; these are detailed in [15,22], so will not be discussed here. The NOx concentrations measured at the kerb were higher and fluctuated more than those observed at the elevated (1.5 m) sensor node LH. Such observations were in line with earlier studies [23].

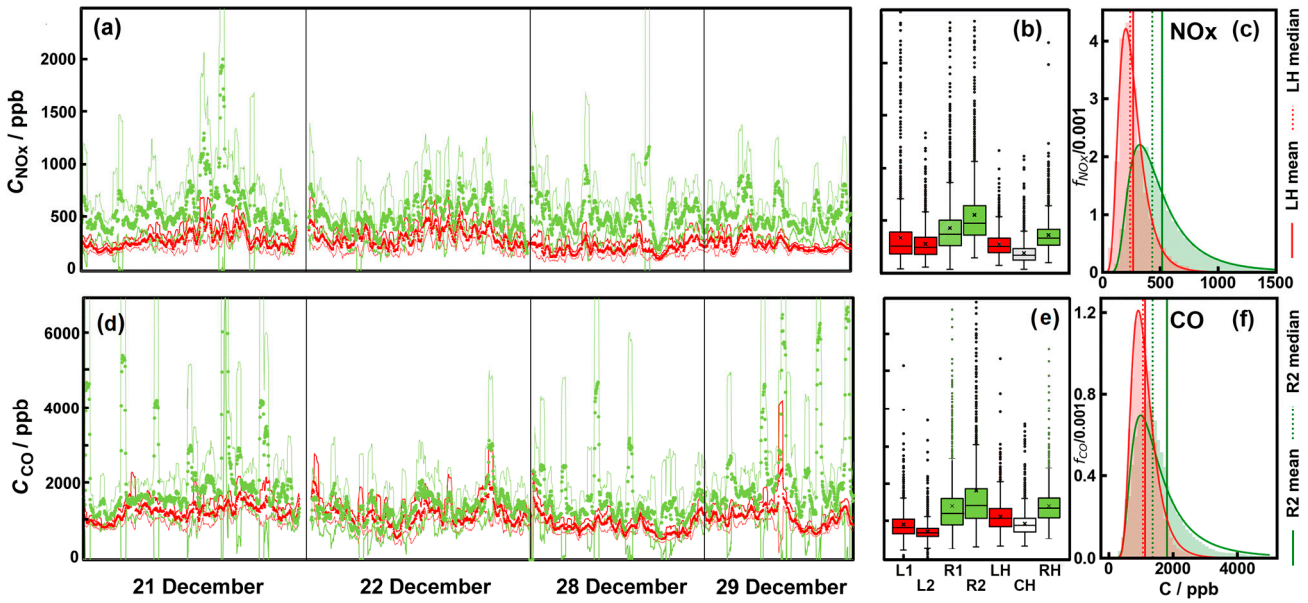

Figure 3. (**a**) One-minute concentrations of NOx smoothed over 15 min for the four campaigns near the traffic (node R2: green dots) and from the covered kerb (node LH: red triangles appear as a thick line). Thin lines are the boundaries of the standard deviations. (**b**) Box and whisker plots of 1-min average concentrations at the seven nodes. Note: the boxes define quartiles Q_1 and Q_3, the median is denoted with a line and the mean by "x". (**c**) The 1-s NOx concentrations from nodes LH and R2 fitted to a Weibull distribution. (**d**) One-minute concentrations of CO smoothed over 15 min for node R2 (green dots) and LH (red triangles appear as a thick line) over the four days. Thin lines are the boundaries of the standard deviations. (**e**) Box and whisker plots of 1-min average concentrations of CO at the seven nodes. (**f**) The 1-s CO concentrations from nodes LH and R2 fitted to a Weibull distribution.

The 1-s-interval measurements of the NOx concentrations from the seven sites over the four days of the campaign are summarised in Figure 3b. The pollutant concentrations at the left-hand kerb (red L1 and L2) were lower than their right-hand counterparts near the tramway (green R1 and R2). This was because the traffic was obliged to use the right lane. The kerbside values were typically higher than those in the pedestrian environments, including the lamp post on the left (red LH), the overhead pedestrian walkway (white CH) and the stairway (green RH) on the right. These were all further from the traffic pollutant sources.

The mean NOx concentrations at the four kerbside nodes L1, L2, R1 and R2 were 338 ± 311, 282 ± 185, 436 ± 451 and 556 ± 552 ppb, respectively. The values at the lamp post, walkway and staircase were 196 ± 121, 366 ± 168 and 348 ± 332 ppb, respectively. The 1-s-interval data were not normally distributed (Figure 3c). The skewness led to the large standard deviations. Nonetheless, the large sample size allowed the use of ANOVA as a test for the difference among the means. The omnibus p-value was very small (<0.0001). Tukey's HSD showed that the NOx concentrations at the lamp post and the stairway were lower than those of the two kerbside nodes on the left of the carriageway ($p < 0.01$).

The skewed concentration data exhibited a Weibull distribution, with a scale parameter λ_{NOx} = 6.98 for kerbside node R2 and λ_{NOx} = 68 for the elevated node LH. The shape parameter was k_{NOx} = 0.41 for node R2 and k_{NOx} = 0.87 for the elevated node LH. The lower value at R2 was an indicator of greater skewness. The skewed data, especially in the kerbside measurements, were the consequence of vehicular exhaust. The scale parameters for the kerbside nodes ranged from 0.30 to 0.46, but were larger (0.63 to 0.70) for the elevated nodes, reflecting more normal distributions.

The CO concentrations are plotted in Figure 3d,e. The mean concentrations at the four kerbside nodes (L1, L2, R1 and R2) were 925 ± 399, 744 ± 233, 1418 ± 982 and 1837 ± 2007 ppb, respectively. The values at the lamp post (LH), walkway (CH) and stairs

(RH) were 1146 ± 415, 948 ± 350 and 1420 ± 483 ppb, respectively. Curve fitting to Weibull distribution gave the shape parameter k_{CO} = 0.29 for kerbside R2 and k_{CO} = 0.82 for the elevated node LH. The lower value at R2 again indicated a greater skewness at the kerb. The two pollutants revealed rather similar shape parameters (k_{NOx} = 0.86 and k_{CO} = 0.82). This in turn hinted that the distribution of both NOx and CO at the elevated sites was influenced by mixing with air aloft, such that the central tendency led to concentration distributions that appeared closer to normal.

3.3. Autocorrelation and Cross-Correlation

Air pollutant concentrations can be highly correlated [24], though most earlier work has typically been concerned with longer time intervals (hours and days) rather than seconds. Pavageau and Schatzmann [2] note that autocorrelation persists in the stagnant zones of air that lie outside the vortices in urban canyons. In our measurements, the autocorrelation persisted for almost a minute with $r^2 > 0.75$ at the footbridge above the carriageway and at the elevated nodes on either side of the carriageway (LH and RH). In the areas being affected by the wakes of passing traffic, most notably at the sampling nodes on the right-hand side of the carriageway (R1 and R2), autocorrelation declined rapidly.

Autocorrelation of 1-s NOx concentrations at nodes R1 and R2 generally showed a rapid decline (Figure 4a–d). As the nodes on the right-hand side (RHS) of the carriageway with the most active traffic flow, they were understandably the most turbulent. Node L2 on the less turbulent left-hand lane often showed a decline that was slower than that of nodes R1 and R2. The autocorrelation function at the more elevated nodes LH, CH and RH also decayed more slowly; this was probably associated with less turbulent air and less variation in pollutant concentrations. The average autocorrelation of 1-s CO concentrations across the four days is shown in Figure 4e. It was more persistent at the elevated site on the walkway, suggesting that the CO concentrations did not fluctuate rapidly. This in turn implied a larger contribution from better-mixed canyon air. However, a greater NOx fluctuation was observed at this node because of the varying contributions from traffic sources.

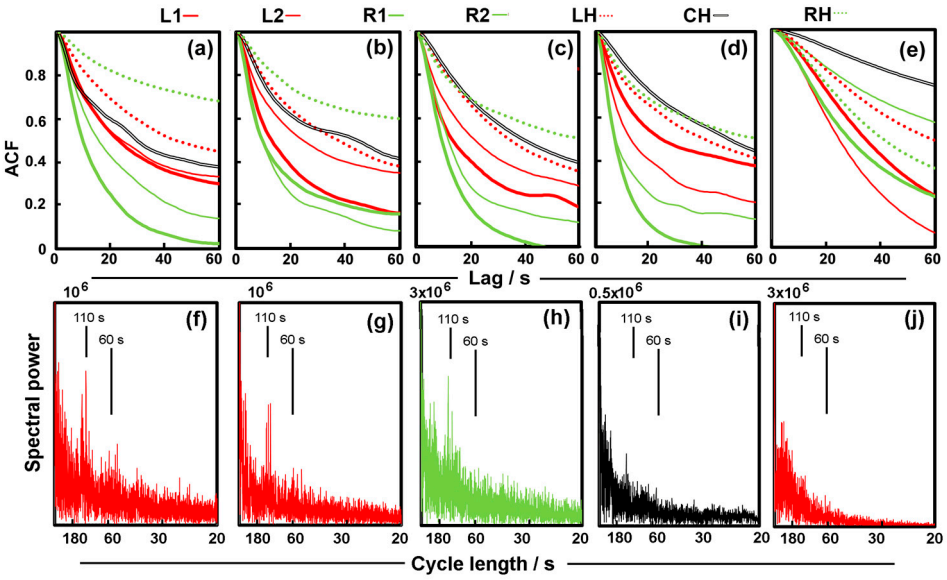

Figure 4. The autocorrelation function (ACF) of 1-s NOx concentrations for the seven nodes for the four days: (**a**) 12–21, (**b**) 12–22, (**c**) 12–28 and (**d**) 12–29. (**e**) Average autocorrelation of 1-s CO across the four nodes for the entire campaign. Fourier transforms for NOx on 12–21 at the kerbside nodes, (**f**) L1, (**g**) L2 and (**h**) R2, and the elevated node on the overhead walkway (**i**) CH, along with the transform for (**j**) kerbside CO at L1. Note the spectral power takes the units ppb^2 Hz^{-1}, with the quantity at the top of each figure (**f**–**j**) shown by the small numerals.

The time traces of the concentrations were examined for lower frequencies using Fourier analysis, which revealed weak cycles at 60 and 110 s (Figure 4f–j). Although only some of the times series from December of 2021 were displayed, these cycles were found on most days at the four kerbside nodes for NOx. These two cyclic periods were clearest in the data from node L1, which was close to the crossroad of Percival Street and Hennessy Road. Hong Kong uses an Adaptive Traffic System (SCATS), which coordinates the lights according to the traffic conditions. Generally, the vehicles in Percival Street wait for a 60-s green light, then go straight ahead or turn left. The traffic flow along Hennessy Road followed another cycle of 110 s. These timings fit closely with those shown in the Fourier transforms (Figure 4g–j). However, the evidence of periodicity was weaker further along the road at nodes L2 and R2, especially for the 60-s cycle. The cycles were perhaps just evident for the 110-s cycle at the overhead walkway RH (Figure 4i). The time series for CO, even at the crossroad node L1, revealed little evidence of cycles. Although there was some hint of another longer cycle of a 4 min duration (Figure 4j), it remains unexplained. Nevertheless, these observations suggested that traffic management leaves a signature in the times series of primary pollutant concentrations at the canyon bottom.

Cross-correlation analysis has proved to be of value in understanding how airflow may vary between an enclosed portion of a canyon and intersections [25]. Here, we used cross-correlation to explore the lags between the appearance of pollutants at various locations, with node R1 taken as the reference (Figure 5a). Across the entire campaign, the cross-correlation functions were slightly delayed at the other nodes. A similar picture emerged for CO (Figure 5b). The lag time was longer for the elevated nodes (Figure 4c), suggesting that the pollutant signal moved more slowly in the vertical direction. The signals, and presumably the pulses of exhaust pollutants [22], moved more rapidly in the horizontal direction, as the kerbside nodes were separated by less than 10 m, representing just a few seconds of vehicles travel along Hennessy Road. However, it took slightly longer for the concentration signal to cross the carriageway from the right-hand kerb to that on the left (nodes L1 and L2). The signal took some tens of seconds to reach the elevated nodes, e.g., the signal observer on the walkway (CH) was often delayed by more than 20 s.

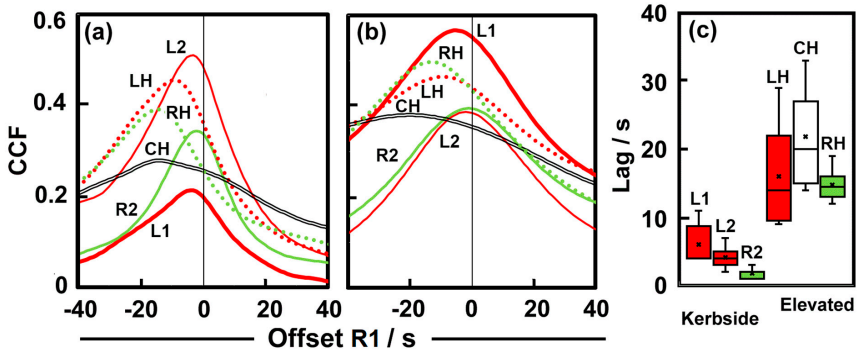

Figure 5. (**a**) The cross-correlation function (CCF) of 1-s NOx concentrations from the other six nodes with R1 on 12–28 and (**b**) CO. (**c**) The lag of each node for both NOx and CO with node R1 determined for the four days.

3.4. Wind Speed and Pollutant Concentration

There is often an inverse relationship between wind speed and pollutant concentration (Figure 6); this has long been a part of the understanding of the distribution of air pollutant concentrations [26] and has been incorporated into canyon models [21]. Separating the data from each of the nodes into 1-min periods when the wind was less than 1 m·s^{-1} (measured at node L2) and periods of stronger winds showed that there was usually a weak but significant (*t*-test: $p < 0.001$) inverse relationship between NOx and the wind speed. While it was insignificant for NOx, the relationship for CO at nodes L1 and R2 was notably weakened at higher wind speeds. However, the effect was modest, as the wind

speeds remained low at the canyon base; there was a 10–20% decrease in CO and a less consistent change in NOx, ranging between a 20% decrease and a non-significant increase of 4% at node L1.

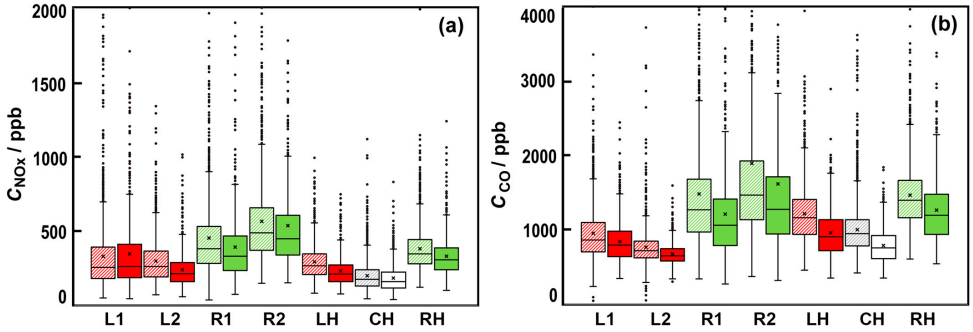

Figure 6. (**a**) The 1-min NOx concentrations when the 1-min average wind speed was <1.0 or ≥1.0 m·s^{-1} in the 4-day campaign. Note: The hatched shading is for winds <1.0 m·s^{-1}. (**b**) The average concentration of CO when 1-min average wind speed was <1.0 or ≥1.0 m^{-1} in the 4-day campaign.

3.5. Nitrogen Oxide Transformations

The oxidation of NO to NO_2 is rapid, taking only minutes [11]. It is relevant to the canyon environment [27], though likely to be constrained at the canyon bottom. Here, O_3 is typically depleted through reaction with NO, which limits the amount of NO_2 that can be produced. In remote areas of Hong Kong, e.g., the island of Tap Mun, most of the small amount of NOx (~6 ppb) is oxidized to NO_2 (~85%) [28]. Even though it is at the roadside, a significant fraction ($f_{NO2} = C_{NO2}/C_{NOx}$) of the NOx could be oxidized at the Causeway Bay monitoring station when the O_3 concentrations were high (Figure 7). However, over the same period, the amount of NO oxidized at the kerb (node R2) was much smaller, showing only a weak dependence on the O_3 concentrations at the Causeway Bay MTR Station. The kerbside environment had little O_3, so there was limited potential for the oxidation of a substantial amount of NO. The slight positive slope at node R2 hinted that NO_2 was formed in these environments, but it was probably limited by the available O_3.

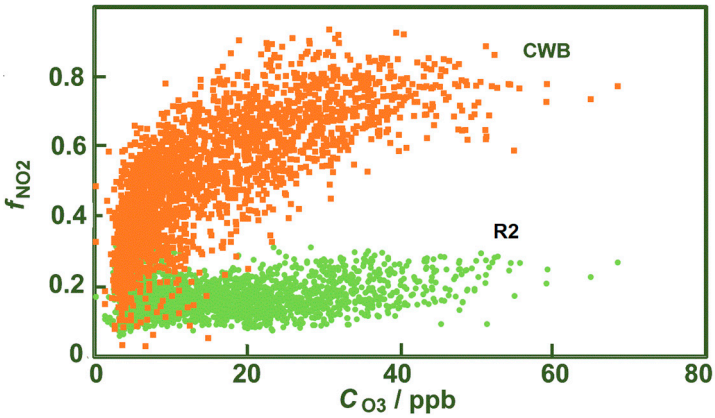

Figure 7. The fraction of NO_2 (f_{NO2}) at node R2 and the Causeway Bay monitoring station (CWB) at 1-min intervals across the four days as a function of the concentration of ozone (C_{O3}) measured at the monitoring station.

3.6. Exposure at the Kerb

The roadside near the sampling site was busy. Node LH was less than 10 m from Causeway Bay MTR Station Exit B, which is part of the Island Line, carrying close to a million passengers a day. The weak winds and poor dispersion at the canyon base enhance

the pollutant concentrations. These may vary widely, as they are affected by flows along the canyon, segments of vehicle plumes and turbulent wakes. The NO_2 concentrations could also vary because of changes in the rate of NO oxidation in response to O_3 variations.

These rapid changes in concentration may complicate contributions to pedestrian exposure, given the brevity of typical pedestrian occupancy at the roadside. It is clear that pedestrians are exposed to highly variable environments. In Hong Kong, there may be sustained roadside exposures for the street traders, transport officials or even picnicking domestic workers who often occupy Hong Kong's near-road environment on Sundays. It has been common to integrate the short-term exposures over a day [29,30]. Hong Kong's *Air Quality Health Index* [31] is based on a three-hour rolling average, which would again lessen the impact of the brief extreme exposures detected in this study over minutes or seconds.

The Hong Kong Air Quality Objectives hourly guideline value for NO_2 is 100 ppb. During the 45 h of the campaign, which covered the busiest times, the hourly average NO_2 concentration at node LH was 77 $\pm$ 8.9 ppb. It never exceeded the guideline, though the maximum was 91.6 ppb. However, across the campaign period, 100 ppb was exceeded for 100 min and the maximum value was 158 ppb over a minute. Naturally, it was much worse at the kerb, and on five occasions the hourly average of NO_2 concentration exceeded 100 ppb. Overall, the hourly NO_2 concentrations were 84 $\pm$ 15.7 ppb (maximum 138 ppb) at node R2, where guideline level of NO_2 was exceeded for 348 min, with a maximum concentration of 2735 ppb. It may seem unlikely that pedestrians would be positioned at this sampling inlet, breathing just 40 cm above the road; however, it should be noted that the tram stop is near the right-side lane of traffic, so people waiting to catch a tram would be exposed to elevated pollutant concentrations. It is not clear that simply integrating multiple short, high-concentration exposures really captures the health risks. Rom et al. [32] observe that "short exposure times, single or limited exposures . . . cannot model the multipollutant exposure of the real world, and the difficulty of separating the physiological effects of exercise from the effects of air pollutants".

4. Summary and Conclusions

This study examined the rapid, spatiotemporal variation in the concentrations of NOx and CO at the base of a confined urban street canyon, the result of heavy traffic, weak winds and the poor dispersion of primary pollutants. Turbulence and pulses of pollutants from passing vehicles caused a rapid variation in the concentrations, which could be extremely high for brief periods. More persistent autocorrelation was observed in the less turbulent air at the sampling nodes elevated to a few metres, while cross-correlation showed that the pollutant signals took from 10 to 30 s to reach these places. The cross-correlation declined more rapidly along the road (horizontally) than vertically, implying that the pulses of pollutants were readily transferred by vehicle movement and horizontal advection. The management of vehicle flow by traffic lights imposed a cyclic signature to the pollutant signal that related to the signal timings. The wind speeds, though slow at the canyon bottom, reduced the pollutant concentrations. The much-depleted ozone concentrations at exhaust level reduced the potential for NO_2 production, which is a topic worthy of further research.

Pollutants at the canyon bottom are heterogeneous, but it is a place frequently crowded with pedestrians who are exposed to rapidly changing concentrations. At the middle of the dual carriageway, high pollutant concentrations can be experienced, so Hong Kong's tram stops are relevant places to study. Additionally, chemical reactions add to the rapid variation in street-level NO_2. They could also lead to varying amounts of nanoparticles and reactive oxygen species (ROS), making pedestrian exposures complex. Although pedestrians are likely to dwell on the pavement for only short periods, the relevance of brief exposure to extreme pollutant concentrations is not well understood. It would be of benefit if this could be properly incorporated into cumulative exposure estimates.

The heterogeneity in the first few metres of an urban canyon makes pollution in this microenvironment relevant yet complicated to resolve.

Author Contributions: M.-Y.C., undertaking fieldwork, data analysis and management, draughting figures; P.B., conceptualisation, data analysis, original draft and final editing, draughting figures; C.-H.L., review; Z.N., initiating investigation, supervision, methodology, review. All authors have read and agreed to the published version of the manuscript.

Funding: European Union (EU)–Hong Kong Research and Innovation Cooperation Co-funding Mechanism by the Research Grants Council (RGC Ref.: E-HKUST601/19), Collaborative Research Fund (CRF) for 2018/19 (RGC Ref No. C7064-18G) and Hong Kong Environment and Conservation Fund (ECF/19/2018) and Ministry of Science and Technology, Taiwan: MOST 110-2621-M-110-009.

Data Availability Statement: Third Party Data restrictions apply to the availability of these data.

Conflicts of Interest: The authors declare no conflict of interest. The funders helped with access to and use of the site chosen for the campaign but had no role in the analysis and interpretation of data or decisions related to this manuscript.

References

1. Kamara, A.A.; Harrison, R.M. Analysis of the air pollution climate of a central urban roadside supersite: London, Marylebone Road. *Atmos. Environ.* **2021**, *258*, 118479. [CrossRef]
2. Pavageau, M.; Schatzmann, M. Wind tunnel measurements of concentration fluctuations in an urban street canyon. *Atmos. Environ.* **1999**, *33*, 3961–3971. [CrossRef]
3. Duan, G.; Brimblecombe, P.; Chu, Y.L.; Ngan, K. Turbulent flow and dispersion inside and around elevated walkways. *Build. Environ.* **2020**, *173*, 106711. [CrossRef]
4. Vardoulakis, S.; Fisher, B.E.; Pericleous, K.; Gonzalez-Flesca, N. Modelling air quality in street canyons: A review. *Atmos. Environ.* **2003**, *37*, 155–182. [CrossRef]
5. Ngoc, L.T.N.; Kim, M.; Bui, V.K.H.; Park, D.; Lee, Y.C. Particulate matter exposure of passengers at bus stations: A review. *Int. J. Environ. Res. Public Health* **2018**, *15*, 2886. [CrossRef]
6. Abhijith, K.V.; Kumar, P. Field investigations for evaluating green infrastructure effects on air quality in open-road conditions. *Atmos. Environ.* **2019**, *201*, 132–147. [CrossRef]
7. Buccolieri, R.; Jeanjean, A.P.; Gatto, E.; Leigh, R.J. The impact of trees on street ventilation, NOx and PM2. 5 concentrations across heights in Marylebone Rd street canyon, central London. *Sustain. Cities Soc.* **2018**, *41*, 227–241. [CrossRef]
8. Kumar, P.; Zavala-Reyes, J.C.; Tomson, M.; Kalaiarasan, G. Understanding the effects of roadside hedges on the horizontal and vertical distributions of air pollutants in street canyons. *Environ. Int.* **2022**, *158*, 106883. [CrossRef]
9. Lo, K.W.; Ngan, K. Characterizing ventilation and exposure in street canyons using Lagrangian particles. *J. Appl. Meteorol. Clim.* **2017**, *56*, 1177–1194. [CrossRef]
10. Yu, Y.T.; Xiang, S.; Noll, K.E. Evaluation of the Relationship between Momentum Wakes behind Moving Vehicles and Dispersion of Vehicle Emissions Using Near-Roadway Measurements. *Environ. Sci. Technol.* **2020**, *54*, 10483–10492. [CrossRef]
11. Palmgren, F.; Berkowicz, R.; Hertel, O.; Vignati, E. Effects of reduction of NOx on the NO_2 levels in urban streets. *Sci. Total Environ.* **1996**, *189*, 409–415. [CrossRef]
12. Rakowska, A.; Wong, K.C.; Townsend, T.; Chan, K.L.; Westerdahl, D.; Ng, S.; Močnik, G.; Drinovec, L.; Ning, Z. Impact of traffic volume and composition on the air quality and pedestrian exposure in urban street canyon. *Atmos. Environ.* **2014**, *98*, 260–270. [CrossRef]
13. HKEPD. Hong Kong Emission Inventory Report, Environmental Protection Department, The Government of HKSAR. Available online: https://www.epd.gov.hk/epd/sites/default/files/epd/data/2019%20Emission%20Inventory%20Report_Eng.pdf (accessed on 14 December 2021).
14. Wong, P.P.Y.; Lai, P.-C.; Allen, R.; Cheng, W.; Lee, M.; Tsui, A.; Tang, R.; Thach, T.-Q.; Tian, L.; Brauer, M.; et al. Vertical monitoring of traffic-related air pollution (TRAP) in urban street canyons of Hong Kong. *Sci. Total Environ.* **2019**, *670*, 696–703. [CrossRef] [PubMed]
15. Chu, M.; Brimblecombe, P.; Wei, P.; Lee, K.C.C.; Yat, Y.S.; Liu, C.-H.; Ning, Z. Kerbside NOx and CO concentrations and emission factors of vehicles on a busy road. *Atmos. Environ.* **2021**, accepted for publication.
16. Gov HKSAR. Tightened Emission Requirements of Franchised Bus Low Emission Zones to Euro V Standard Take Effect Today (31 December 2019). Available online: https://www.info.gov.hk/gia/general/201912/31/P2019123100268.htm (accessed on 21 November 2021).
17. Wang, H.; Brimblecombe, P.; Ngan, K. A numerical study of local traffic volume and air quality within urban street canyons. *Sci. Total Environ.* **2021**, *791*, 148138. [CrossRef]
18. Zong, H.; Brimblecombe, P.; Sun, L.; Wei, P.; Ho, K.F.; Zhang, Q.; Cai, J.; Kan, H.; Chu, M.; Che, W.; et al. Reducing the influence of environmental factors on performance of a diffusion-based personal exposure kit. *Sensors* **2021**, *21*, 4637. [CrossRef]

19. Wessa, P. Free Statistics Software, Office for Research Development and Education, 2021 Version 1.2.1, URL. Available online: https://www.wessa.net/ (accessed on 13 December 2021).
20. Jeong, S.J.; Andrews, M.J. Application of the k–ε turbulence model to the high Reynolds number skimming flow field of an urban street canyon. *Atmos. Environ.* **2002**, *36*, 1137–1145. [CrossRef]
21. Vardoulakis, S.; Gonzalez-Flesca, N.; Fisher, B.E.; Pericleous, K. Spatial variability of air pollution in the vicinity of a permanent monitoring station in central Paris. *Atmos. Environ.* **2005**, *39*, 2725–2736. [CrossRef]
22. Chu, M.; Brimblecombe, P.; Wei, P.; Ning, Z. Temporal structure of vehicle exhaust plumes in the kerbside environment. *Sci. Total Environ.* **2021**. submitted.
23. Karra, S.; Malki-Epshtein, L.; Neophytou, M.K.-A. Air flow and pollution in a real, heterogeneous urban street canyon: A field and laboratory study. *Atmos. Environ.* **2017**, *165*, 370–384. [CrossRef]
24. Milionis, A.E.; Davies, T.D. Regression and stochastic models for air pollution—I. Review, comments and suggestions. *Atmos. Environ.* **1994**, *28*, 2801–2810. [CrossRef]
25. Richmond-Bryant, J.; Eisner, A.D.; Hahn, I.; Fortune, C.R.; Drake-Richman, Z.E.; Brixey, L.A.; Talih, M.; Wiener, R.W.; Ellenson, W.D. Time-series analysis to study the impact of an intersection on dispersion along a street canyon. *J. Environ. Monit.* **2009**, *11*, 2153–2162. [CrossRef]
26. Bencala, K.E.; Seinfeld, J.H. On frequency distributions of air pollutant concentrations. *Atmos. Environ.* **1976**, *10*, 941–950. [CrossRef]
27. Kwak, K.H.; Baik, J.J. Diurnal variation of NOx and ozone exchange between a street canyon and the overlying air. *Atmos. Environ.* **2014**, *86*, 120–128. [CrossRef]
28. HKEPD. Air Quality in Hong Kong 2020 Statistical Summary, Air Science Group. Available online: https://www.aqhi.gov.hk/api_history/english/report/files/2020StatSum_en.pdf (accessed on 14 December 2021).
29. Bates, D.V.; Bell, G.; Burnham, C.; Hazucha, M.; Mantha, J.; Pengelly, L.D.; Silverman, F. Problems in studies of human exposure to air pollutants. *Can. Med. Assoc. J.* **1970**, *103*, 833.
30. Ott, W.R. Total human exposure. *Environ. Sci. Technol.* **1985**, *19*, 880–886. [CrossRef]
31. GovHK. Air Quality Health Index. Hong Kong Special Administrative Region Government. 2014. Available online: http://www.gov.hk/en/residents/environment/air/aqhi.htm (accessed on 3 June 2021).
32. Rom, W.N.; Boushey, H.; Caplan, A. Experimental human exposure to air pollutants is essential to understand adverse health effects. *Am. J. Respir. Cell Mol. Biol.* **2013**, *49*, 691–696. [CrossRef]